

# Ion mobility-high resolution mass spectrometry (IM-HRMS) for the analysis of Contaminants of Emerging Concern (CECs): Database compilation and application to urine samples

Lidia Belova<sup>1\*</sup>, Noelia Caballero-Casero<sup>1,&</sup>, Alexander L.N. van Nuijs<sup>1\$</sup>, Adrian Covaci<sup>1\$\*</sup>

*1 - Toxicological Centre, University of Antwerp, Universiteitsplein 1, 2610, Antwerp, Belgium*

\* - corresponding authors (Lidia Belova: [Lidia.Belova@uantwerpen.be](mailto:Lidia.Belova@uantwerpen.be); Adrian Covaci: [Adrian.Covaci@uantwerpen.be](mailto:Adrian.Covaci@uantwerpen.be))

\$ - shared last authors

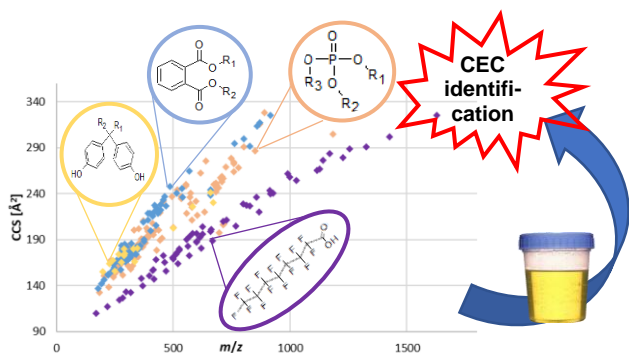
& - current address; Department of Analytical Chemistry, Nutrition and Food Science. University of Salamanca, Salamanca, 37008 Spain

## Abstract

Ion mobility mass spectrometry (IM-MS)-derived collision cross section (CCS) values can serve as a valuable additional identification parameter within the analysis of compounds of emerging concern (CEC) in human matrices. This study introduces the first comprehensive database of <sup>DT</sup>CCS<sub>N<sub>2</sub></sub> values of 148 CECs and their metabolites including bisphenols, alternative plasticizers (AP), organophosphate flame retardants (OP), perfluoroalkyl chemicals (PFAS), and others. A total of 311 ions were included in the database, whereby the <sup>DT</sup>CCS<sub>N<sub>2</sub></sub> values for 113 compounds are reported for the first time. For 105 compounds, more than one ion is reported. Moreover, the <sup>DT</sup>CCS<sub>N<sub>2</sub></sub> values of several isomeric CECs and their metabolites are reported to allow a distinction between isomers. Comprehensive quality assurance guidelines were implemented in the workflow of acquiring <sup>DT</sup>CCS<sub>N<sub>2</sub></sub> values to ensure reproducible experimental conditions. The reliability and reproducibility of the compiled database were investigated by analyzing pooled human urine spiked with 30 AP and OP metabolites at two concentration levels. For all investigated metabolites, the <sup>DT</sup>CCS<sub>N<sub>2</sub></sub> values measured in urine showed a percent error of <1% in comparison to database values. <sup>DT</sup>CCS<sub>N<sub>2</sub></sub> values of OP metabolites showed an average percent error of 0.12% (50 ng/mL in urine) and 0.15% (20 ng/mL in urine). For AP metabolites, these values were 0.10 and 0.09%, respectively. These results show that the provided database can be of great value for enhanced identification of CECs in environmental and human matrices, which can advance future suspect screening studies on CECs.

**Keywords:** ion mobility; high-resolution mass spectrometry; collision cross section; CCS database; contaminants of emerging concern; urine

## Graphical Abstract



## Introduction

In recent years, the increasing number of reports of contaminants of emerging concern (CECs) presents a growing potential hazard for ecological and human health<sup>1-3</sup>. The group of CECs includes plasticizers (phthalates, terephthalates, benzoates, sebacates, etc.), brominated and organophosphorus flame retardants, antioxidants and UV-light stabilizers, and other chemicals. CECs are not extensively included in (bio)monitoring programs, because they have very recently been identified or their toxic effects or influence on the environment and humans are not yet well understood<sup>4</sup>. The high structural variety and number of CECs present an additional challenge for biomonitoring methods<sup>5</sup>.

Target analytical methods commonly used in biomonitoring studies focus on detecting a limited number of *a priori* selected environmental contaminants. While this approach is highly important for quantitative data collection and assessment of human exposure to known contaminants, it cannot address the rising issue of CECs. In contrast, non-target and suspect screening methods, which underwent a strong development during the last decade<sup>6, 7</sup>, allow the simultaneous detection of numerous analytes by high-resolution mass spectrometry (HRMS) as detection technique<sup>8, 9</sup>.

Within both analytical approaches, the identification of detected compounds marks a crucial point in obtaining reliable results and interpreting them<sup>5</sup>. Schymanski et al. proposed a harmonized system to report compound identification levels ranging from level 5 (only exact mass available) to level 1 (confirmation with reference standard)<sup>10</sup>. Within suspect and non-target screening, a confidence level of up to 2 can be reached if fragmentation data (i.e. MS/MS spectra) of the detected compounds is available and can be matched with databases. However, within the field of CECs analysis, the unavailability of high-quality reference MS/MS spectra can limit compound identification. Even though in recent years high emphasis is put on the expansion of MS/MS spectral libraries, a further harmonization, the inclusion of emerging and recently discovered compounds, as well as the

implementation of uniform QA/QC measures, are still required<sup>11</sup>. These actions are especially needed to increase the harmonization of MS/MS spectra between different mass spectrometric instrumentation and laboratories, which at the moment poses a major challenge within non-target and suspect screening<sup>11</sup>. Even if matching MS/MS spectra are available, very low concentrations of CECs in biological samples and coeluting matrix components can hamper MS/MS spectra acquisition and compromise their quality by producing low abundant fragment spectra which are difficult to interpret<sup>12</sup>. Furthermore, generic liquid chromatography methods commonly used within suspect and non-target screening show limited separation capabilities for structurally similar, isobaric or isomeric compounds leaving potential new CECs undetected and emphasizing the need for additional separation space<sup>5, 13</sup>.

Ion mobility mass spectrometry (IM-MS) provides an additional separation dimension for suspect and non-target analyses. Drift tube ion mobility spectrometry (DTIMS) is based on the rapid conformational separation of ions depending on their size, shape, charge state and thereof resulting gaseous mobility. After ionization in the ion source and prior to pulsing ion packages into the drift tube, ions are accumulated and focused within a tandem ion funnel interface. The subsequent drift tube operates under a low uniform electrical field (typically 5 - 100 Vcm<sup>-1</sup>) and is filled with a buffer gas at a pressure of about 525 Pa<sup>14</sup>. While traveling through the drift tube, ions undergo collisions with the buffer gas molecules which exert a dragging force determining the ions' specific drift times. A maximum drift time (i.e. time between ion pulses) must be set to define the duration of the ion-mobility analysis cycle (i.e. frame). While the standard instrumental set-up includes one ion pulse per frame, ion multiplexing allows multiple ion pulses per frame whereby trap filling and release are modulated based on a 3-bit or 4-bit pseudorandom binary sequence (PRS). This approach requires significantly lower trap filling times leading to decreased space-charge effects within the front funnel interface<sup>15</sup>. Additionally, it allows an increased ion utilization resulting in a higher number of data points per peak and an improved sensitivity of up to 9-fold<sup>15, 16</sup>.

Ultimately, IM-HRMS allows the determination of the drift time and mass-to-charge ratio ( $m/z$ ) for each detected feature. This information is used to calculate compound specific collision cross section (CCS) values describing the rotationally averaged surface (in Å<sup>2</sup>) of the ion<sup>17</sup>. The CCS value represents a compound specific physiochemical descriptor which can serve as an additional identification parameter within feature annotation and compound identification<sup>18</sup>. This can decrease the number of false positives since a distinction between features with identical  $m/z$  ratios and retention times is possible<sup>19</sup>. The observation of various adducts per compound which is facilitated by the additional separation dimension further increases the number of identification parameters<sup>20</sup>. Thereby, IM-MS measurements show several advantages since they allow to separate isomeric analytes or coeluting matrix components. Also, interfering phenomena such as carry-over or matrix effects do not occur since the gaseous phase responsible for the separation is being constantly replaced<sup>21</sup>. Furthermore, <sup>DT</sup>CCS<sub>N2</sub> values have shown high intra- and interlaboratory reproducibility supporting the interlaboratory exchange of <sup>DT</sup>CCS<sub>N2</sub> values, provided that sufficient quality assurance and control (QA/QC) are implemented within their acquisition<sup>21, 22</sup>. The reproducibility of <sup>DT</sup>CCS<sub>N2</sub> values was investigated by Stow et al. showing an interlaboratory relative standard deviation (RSD) of 0.30±0.16% after the analysis of 51 biologically relevant standards, such as amino acids and lipids<sup>22</sup>. Further IM-MS studies conducted on human and veterinary drugs (interlaboratory

100 RSDs<0.29%)<sup>20</sup>, drugs and structurally related compounds (intralaboratory interday RSDs<0.5%)<sup>23</sup> and pesticides  
101 (intralaboratory intraday RSDs<0.5% for 96% of the analyzed compounds)<sup>24</sup> confirm the utility of CCS values as  
102 a reproducible complementary identification parameter.

103

104 However, for the use of IM-MS data for compound identification, the compilation of comprehensive databases  
105 containing CCS values of the compounds of interest is essential. In the past, the focus of available databases was  
106 on endogenous compounds, such as peptides<sup>25</sup>, glycans<sup>26</sup>, lipids<sup>27</sup>, steroids<sup>28</sup> reflecting that omics-based studies  
107 in different fields, such as metabolomics<sup>29, 30</sup>, lipidomics<sup>31, 32</sup>, plantomics<sup>33</sup> or proteomics<sup>34</sup> have been the  
108 predominant recent application of IM-MS. Yet, interest in the use of IM-MS for the analysis of CECs is rising. Few  
109 studies on the characterization of per- and polyfluoroalkyl substances (PFAS)<sup>35-37</sup> or organophosphorus flame  
110 retardants (OPs)<sup>38</sup> using IM-MS have been reported and few databases containing CCS values of xenobiotics  
111 have been introduced in the past <sup>39, 40</sup>.

112 Nevertheless, a comprehensive database covering a broad range of CECs from different classes is still lacking.  
113 Therefore, in this study we introduce an innovative database containing <sup>DT</sup>CCS<sub>N2</sub> values of more than 140 CECs  
114 (including PFAS, OPs, bisphenols, (alternative) plasticizers and other chemicals) and their metabolites analyzed  
115 using DTIMS in positive and negative polarity modes. The acquisition of <sup>DT</sup>CCS<sub>N2</sub> values followed the guidelines  
116 for QC proposed by Picache et al.<sup>21</sup> which ensure data reproducibility and allow data submission to the Unified  
117 CCS Compendium for further use by the scientific community. As a proof of concept, human urine spiked with a  
118 range of CECs was analyzed to investigate the influence of matrix effects on the reproducibility of <sup>DT</sup>CCS<sub>N2</sub> values.  
119 To our knowledge, this is the first study applying multiplexing IM-MS to the analysis of CECs in human samples.

120

## 121 **Materials and methods**

### 122 **Chemicals**

123 All organic solvents used in this study were of LC-grade. Methanol (MeOH), acetonitrile (ACN) and formic acid  
124 (FA) were purchased from Biosolve BV (Valkenswaard, the Netherlands) (≥99.9%). A PURELAB Flexsystem was  
125 used to obtain ultrapure water (18.2 MΩ cm, Milli-Q, Millipore). Ammonium acetate was purchased from Sigma-  
126 Aldrich (eluent additive for LC-MS). The sources from which reference standards of the compound classes  
127 included in the <sup>DT</sup>CCS<sub>N2</sub> database were acquired are summarized in Table S1.

128 Except for PFAS, individual solutions of all standards were prepared in methanol at a concentration of 1 ng/μL.  
129 Native PFAS were available as a mixture at a concentration of 200 pg/μL in methanol.

### 130 **DTIMS conditions**

131 Within this study, all measurements were conducted using an Agilent 6560 drift tube ion-mobility quadrupole time-  
132 of-flight mass spectrometer (DTIM-QTOF MS; Agilent Technologies, Santa Clara, USA). For both positive and  
133 negative polarity modes, the electrospray ionization (ESI) source was operated using a gas temperature and  
134 sheath gas temperature of 300 °C and 350 °C, respectively. The gas and sheath gas flow were set to 9 L/min and

11 L/min, respectively. The nebulizer pressure was 35 psig and voltages of 3500 V (capillary voltage), 1000 V (nozzle voltage) and 320 V (fragmentor voltage) were applied. IM-MS measurements were conducted using high-purity nitrogen (99.999%) as the drift gas. The gas pressure in the drift tube was maintained at 3.95 Torr resulting in a 0.1 - 0.15 Torr pressure difference in comparison to the funnel trap to ensure drift gas purity. The drift tube settings were based on the parameters proposed by Stow et al.<sup>22</sup> and are summarized in Table S2.

#### CCS measurements of standards

All standards except perfluoroalkyl carboxylic and sulfonic acids (PFCA and PFSA, respectively) which were only available as a mixture were directly injected as separate solutions using the Agilent 1290 Infinity II UPLC connected to the DTIM-QTOF (injection volume 2  $\mu$ L). The mobile phases consisted of water with 2 mM ammonium acetate (A) and methanol (B) for the negative ionization mode. For positive ionization, 0.1% formic acid was added to both mobile phases. These generic conditions provided sufficient ionization for all compounds reported in this database. For direct injections of standards, the mobile phase consisted of 50:50 (v/v) A/B at a flow rate of 0.2 mL/min. The liquid chromatography method applied for the analysis of PFAS mixtures is summarized in Table S3.

Single field calibration was used for all  $^{DT}CCS_{N_2}$  measurements. This approach has been validated in several studies in the past<sup>41, 42</sup> and allows the calculation of  $^{DT}CCS_{N_2}$  values based on a set of reference ions with known  $m/z$  and  $^{DT}CCS_{N_2}$  values, which have to be analyzed under the exact same conditions as the compounds of interest. The ESI low concentration tune mix (Agilent Technologies, Santa Clara, USA) was used as a reference standard and, to ensure instrument stability, was analyzed after every five standards by introducing the mix through the calibrant delivery system of the instrument.

The guidelines for QC of single field  $^{DT}CCS_{N_2}$  measurements proposed by Picache et al.<sup>21</sup> provide a quality assurance (QA) compound list whose  $^{DT}CCS_{N_2}$  values have been acquired with a DTIMS Reference System having the lowest measurement uncertainty to date<sup>22</sup>. From this list, at least 5 compounds must be analyzed within every batch. Thereby, the average absolute percent error of experimental  $^{DT}CCS_{N_2}$  values must be  $\leq 0.5\%$ . The percent error for individual compounds should not exceed 1%. The calculation of the percent error is carried out using equation (1):

$$\text{percent error} = \text{ABS} \left( \frac{(CCS_{\text{experimental}} - CCS_{\text{QA}})}{CCS_{\text{QA}}} \cdot 100 \right) \quad (1)$$

Five QA compounds were injected within every analysis batch. The experimental  $^{DT}CCS_{N_2}$  values of QA compounds were used to ensure reproducible measurement conditions and assess the interday reproducibility of the measurements conducted within this study.

Within every run, reference mass solution was constantly introduced into the ion source using a separate isocratic pump and an additional nebulizer assembly. Prior to any data analysis, this step allowed a recalibration of the raw data using the IM-MS Data File Reprocessing Utility (Version B.08.00, Agilent Technologies) to ensure high mass accuracy.

After recalibration, the data files were demultiplexed using the PNNL PreProcessor (version 2020.03.23), based on the assumption that true signals are present in each segment of the PRS corresponding to a pulse. These

170 signals were searched for and extracted based on a Hadamard Transform algorithm<sup>43</sup>. Subsequently,  $^{DT}CCS_{N2}$   
171 values were calculated from the demultiplexed data applying the single field calibration algorithm within the Agilent  
172 IM-MS Browser (version B.08). The average  $^{DT}CCS_{N2}$  value obtained from five injections as well as the (relative)  
173 standard deviation were exported into the  $^{DT}CCS_{N2}$  database.

174

### 175 **Analysis of spiked urine samples**

176 A “dilute-and-shoot” approach was used for the preparation of (spiked) urine samples<sup>44</sup>. In brief, 1 mL of pooled  
177 urine consisting of urine from five healthy volunteers was spiked with a set of OP and AP metabolites (Table S8  
178 and S9) at two concentration levels (i.e. 20 ng/mL and 50 ng/mL in urine). After a 1:5 dilution with methanol and  
179 centrifugation (5 min at 10000 rpm) the supernatant was frozen overnight. Finally, samples were filtered through  
180 a 0.25  $\mu$ m centrifugal filter and injected into the LC-IM-HRMS. Water was used as a blank sample and spiked  
181 following the same procedure. All samples, including blank urine and water samples, were prepared in triplicate.  
182 All samples were analyzed applying the chromatographic conditions previously developed by Bastiaensen et al.<sup>45</sup>.  
183 OP metabolites were analyzed in both ionization polarities, whilst AP metabolites were only analyzed in negative  
184 polarity since for all AP metabolites  $^{DT}CCS_{N2}$  values for  $[M-H]^-$  ions were available. The ionization and IM-MS  
185 conditions remained the same as described above.

186

### 187 **Results and discussion**

188 The implementation of IM-MS in the analysis of CECs in human matrices requires the creation of comprehensive  
189  $^{DT}CCS_{N2}$  databases to match signals detected in human samples. We have chosen a wide selection of different  
190 classes of CECs to include in our database. In addition, we have added the available metabolites of various parent  
191 compounds. To our knowledge,  $^{DT}CCS_{N2}$  of CEC metabolites have not been reported even though their availability  
192 is vital for the application of IM-MS for human samples. To ensure reproducible conditions while acquiring  $^{DT}CCS_{N2}$   
193 values we implemented the QA guidelines proposed by Picache et al.<sup>21</sup> into our workflow. Furthermore, by  
194 analyzing spiked and non-spiked human urine samples we have shown the applicability of the created database  
195 as well as the reproducibility of  $^{DT}CCS_{N2}$  values in human matrices.

196

### 197 **Reproducibility of CCS values of QA compounds**

198 To ensure high accuracy and monitor the reproducibility of  $^{DT}CCS_{N2}$  values, the analysis of QA compounds was  
199 implemented in the database compilation workflow. The selection of QA compounds was based on the QA  
200 compound list proposed by Picache et al.<sup>21</sup>. The reference  $^{DT}CCS_{N2}$  values of these compounds were previously  
201 determined by Stow et al.<sup>22</sup> using a reference DTIMS system which provided highly reproducible instrumental  
202 conditions.

203 Creatinine, L-cystine, cortisol and glucose were used as QA compounds in positive ionization mode,  
204 pyridoxalphosphate, L-histidine and uric acid in negative ionization mode and L-phenylalanine and L-tyrosine in  
205 both modes, respectively. The  $^{DT}CCS_{N2}$  values of the compounds included in the database were acquired within

four analysis batches in positive ionization mode and five analysis batches in negative ionization mode on different days, respectively. Within every analysis batch, each QA compound was analyzed four times thereby fully implementing all QA guidelines proposed by Picache et al.<sup>21</sup>.

Table 1 shows the average experimental <sup>DT</sup>CCS<sub>N2</sub> values acquired throughout all sample batches. The average <sup>DT</sup>CCS<sub>N2</sub> values of each individual sample batch can be found in Table S4. Considering all experimental <sup>DT</sup>CCS<sub>N2</sub> values of QA compounds, the average percent error in comparison to the literature values is 0.12% in positive ionization mode and 0.08% in negative ionization mode, respectively. The mean percent error of individual compounds ranges between 0.01% and 0.82% (Table S4). The experimental <sup>DT</sup>CCS<sub>N2</sub> values show that the requirements of the QA guidelines provided by Picache et al.<sup>21</sup> are met in all sample batches: In both ionization polarities, the average percent error does not exceed 0.50%. Also, none of the individual compounds showed a percent error > 1% in any of the analyses (see Table S4).

Furthermore, the observed relative standard deviations (RSD) confirm the findings of Stow et al. who had observed an average interlaboratory RSD of 0.38 ± 0.19% for three laboratories and all compounds (n = 65) investigated in the study<sup>22</sup>.

The acquired data shows that the DTIMS system used in this study is highly capable to acquire reproducible and accurate <sup>DT</sup>CCS<sub>N2</sub> values that will be applicable in further studies and laboratories.

**Table 1:** Comparison between experimental <sup>DT</sup>CCS<sub>N2</sub> values (CCS<sub>exp.</sub>) and literature <sup>DT</sup>CCS<sub>N2</sub> values (CCS<sub>lit.</sub>) acquired by Stow et al.<sup>22</sup> for QA compounds throughout all sample batches.

QA compound	Adduct Ion	Theoretical m/z	CCS <sub>exp.</sub> ± SD [Å <sup>2</sup> ]	%RSD	n	CCS <sub>lit.</sub> [Å <sup>2</sup> ]	%Error
Creatinine	[M+H] <sup>+</sup>	114.0662	123.09 ± 0.26	0.21	16	122.98	0.09
Glucose	[M+Na] <sup>+</sup>	203.0526	147.03 ± 0.21	0.15	16	146.94	0.06
Cortisol	[M+H] <sup>+</sup>	363.2166	188.91 ± 0.58	0.31	16	188.34	0.30
	[M+Na] <sup>+</sup>	385.1985	212.43 ± 0.21	0.10	16	212.79	0.17
L-Phenylalanine	[M+H] <sup>+</sup>	166.0863	140.46 ± 0.25	0.18	16	140.3	0.12
	[M-H] <sup>-</sup>	164.0717	139.93 ± 0.37	0.26	20	139.94	0.01
L-Cystine	[M+H] <sup>+</sup>	241.0311	149.39 ± 0.10	0.07	16	149.48	0.06
	[M+Na] <sup>+</sup>	263.0131	151.35 ± 0.19	0.13	16	151.43	0.06
L-Tyrosine	[M+H] <sup>+</sup>	182.0812	145.68 ± 0.22	0.15	16	145.58	0.07
	[M-H] <sup>-</sup>	180.0666	144.43 ± 0.38	0.26	20	144.42	0.01
Pyridoxalphosphate	[M-H] <sup>-</sup>	246.0173	149.42 ± 0.06	0.04	20	149.35	0.04
L-Histidine	[M-H] <sup>-</sup>	154.0622	128.55 ± 0.07	0.05	20	128.83	0.21
Uric acid	[M-H] <sup>-</sup>	167.0211	125.69 ± 0.14	0.11	20	125.55	0.11
Average ESI+							0.12
Average ESI-							0.08

## <sup>DT</sup>CCS<sub>N2</sub> values of contaminants of emerging concern and their metabolites

After demonstrating that the DTIMS system used in this study facilitates the acquisition of accurate and reproducible <sup>DT</sup>CCS<sub>N2</sub> values, DTIMS data for more than 140 CECs from various classes were acquired. The investigated classes included bisphenols (BPs, n=12), triazoles (n=5), thiazoles (n=4), organophosphorus flame retardants (OPs, n=22) and their metabolites (n=15), (alternative) plasticizers (n=15) and their metabolites (n=29), PFAS (n=33) and other chemicals (n=13). Each compound was injected five consecutive times in both ionization polarities and the average <sup>DT</sup>CCS<sub>N2</sub> value of each observed ion was included in the database. Thereby, the data

232 was searched for several ions including  $[M+H]^+$ ,  $[M+Na]^+$ ,  $[2M+H]^+$ ,  $[2M+Na]^+$ ,  $[M-H]^-$ ,  $[2M-H]^-$  and  $[2M-H-CO_2]^-$  for  
233 compounds containing a carboxylic group. This approach followed the goal to provide multiple identification points  
234 for each analyte.

235 The final database contained 311 ions which can be found in Table S5 and S6.  $^{DT}CCS_{N_2}$  values ranged from  
236  $109.53 \text{ \AA}^2$  ( $[M-H-CO_2]^-$  for perfluoro-n-butanoic acid) and  $348.02 \text{ \AA}^2$  ( $[2M+Na]^+$  of butyryl-n-trihexyl citrate). The  
237 observed  $m/z$  ratios ranged from  $m/z$  118.0411 ( $[M-H]^-$  of benzotriazole) and  $m/z$  1626.8891 ( $[2M-H]^-$  of  
238 perfluoro-n-hexadecanoic acid). The average RSD of all  $^{DT}CCS_{N_2}$  measurements was 0.05% whereby RSDs for  
239 individual ions ranged from <0.01% to 0.73%. Comparing the experimental and theoretical  $m/z$  values led to an  
240 overall average mass error of 1.70 ppm. Except for four ions (Table S5) none of the individual measurements  
241 exceeded a mass error of 5 ppm. These results show a high reproducibility of the  $^{DT}CCS_{N_2}$  measurements and are  
242 consistent with the average RSDs observed in previous studies<sup>20</sup>.

243 For 105 out of the 148 compounds, more than one ion was observed (see Figure S1). Moreover, 37 compounds  
244 were detected in both ionization polarities. These results show that the compiled database provides  
245 comprehensive information to be applied under various experimental conditions.

246 Several previous studies have investigated the correlation of  $m/z$  ratios and  $^{DT}CCS_{N_2}$  values of different compound  
247 classes<sup>20, 28, 38, 46</sup>. The observed trendlines can give further information on the elemental composition and shape  
248 of the molecular ions, and can serve as an additional confirmation of a correct data acquisition and interpretation  
249 workflow. For example, for several compounds investigated in this study,  $[M+H]^+$  or  $[M-H]^-$  adducts were detected  
250 which, however, showed drift times identical to the drift times of the corresponding  $[2M+H]^+$  and  $[2M-H]^-$  adducts,  
251 respectively. This indicates a post-drift tube formation of monomer ions from the corresponding dimers<sup>47</sup> which will  
252 be then assigned with an incorrect drift time and thereof  $^{DT}CCS_{N_2}$  value. Prior to erroneously submitting the  
253 resulting incorrect  $^{DT}CCS_{N_2}$  values to the database, plots of  $^{DT}CCS_{N_2}$  values as a function of the  $m/z$  ratios can  
254 reveal such effects.

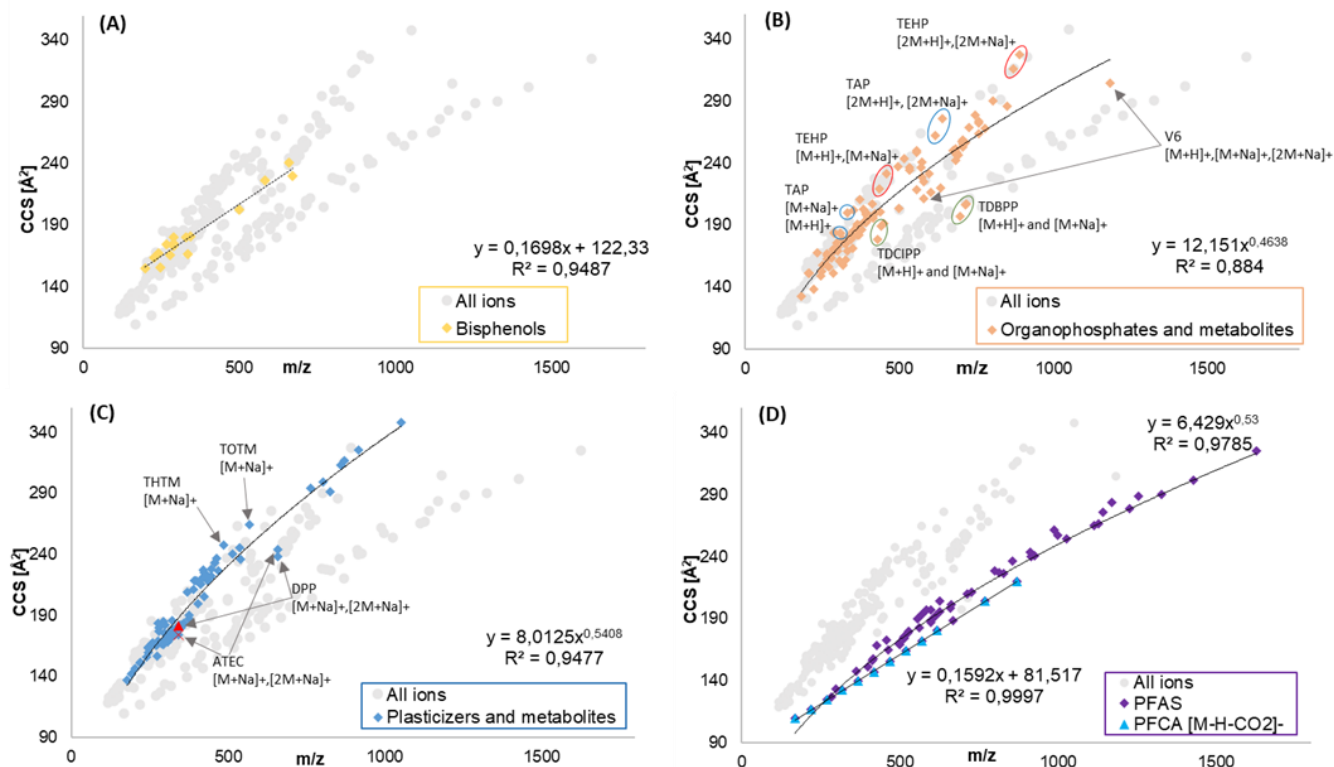


**Figure 1:** Depiction of  $^{DTCCSN_2}$  vs.  $m/z$  for the four main compound classes investigated in this study, including (A) bisphenols (BPs,  $n = 12$ ), (B) organophosphorus flame retardants (OPs) and metabolites ( $n = 37$ ), (C) plasticizers and metabolites ( $n = 38$ ) and (D) PFAS ( $n = 32$ ). Compounds with deviations from the trendlines are indicated: tris(2-ethylhexyl) phosphate (TEHP), triamyl phosphate (TAP), tris(1,3-dichloro-2-propyl) phosphate (TDCIPP), tris(2,3-dibromopropyl) phosphate (TDBPP) and 2,2-bis(chloromethyl)-trimethylene bis(bis(2-chloroethyl)-phosphate) (V6) for OPs and tri-*n*-hexyl trimellitate (THTM), tris(2-ethylhexyl) trimellitate (TOTM), diphenyl phthalate (DPP) and acetyl triethyl citrate (ATEC) for plasticizers. For comparison, all acquired  $^{DTCCSN_2}$  values are displayed in grey.

Figure 1 shows the plots of  $m/z$  ratios and  $^{DTCCSN_2}$  values acquired for the four largest compound groups investigated in this study (BPs, plasticizers and their metabolites, OPs and their metabolites, PFAS). Generally,  $^{DTCCSN_2}$  and  $m/z$  show a non-linear correlation, especially if wide  $m/z$  ranges are considered<sup>48, 49</sup>. However, when evaluating narrower  $m/z$  ranges a linear dependence can provide a better fit<sup>28, 35</sup>.

Bisphenols (Figure 1A) were best fitted applying a linear model resulting in a correlation coefficient ( $R^2$ ) of 0.949. This is consistent with the good linear correlation observed between  $^{DTCCSN_2}$  and  $m/z$  in previous studies<sup>24</sup>.

The  $^{DTCCSN_2}$  values of BPs, OPs and plasticizers cluster in similar areas of the  $^{DTCCSN_2}$  plot. This may be explained by a similar elemental composition of these compound classes, as well as similar molecular shapes.

The relationships between  $^{DTCCSN_2}$  and  $m/z$  values for OPs and their metabolites (Figure 1B) were best fitted applying a power regression model. Still, they showed the lowest correlation coefficient ( $R^2 = 0.882$ ), which is consistent with the highest variability in molecular shapes and elemental compositions of this class. As an example, halogenated OPs, such as TDCIPP, TDBPP and V6, show clearly divergent trends and lower  $^{DTCCSN_2}$  values in comparison to non-halogenated OPs with similar  $m/z$ . Previous studies investigating CCS- $m/z$  trends of halogen-containing compounds observed similar effects<sup>38, 50</sup>. These were assumed to derive from the higher molecular

weight of halogens (F, Cl, Br) in comparison to atoms commonly present in the investigated compound classes (i.e. C, H, O, N, P and S), which results in a lower atom count and thereof in a more compact molecular shape and higher mass density (see Table S5). In contrast, TEHP and TAP show variations from the proposed trend towards increased  $^{DT}CCS_{N2}$  values. Similar effects were observed for the other non-halogenated alkyl OPs and can be described by a separate trendline (Figure S2) showing a better fit ( $R^2=0.983$ ) and a higher slope in comparison to the trendline in Figure 2B. These effects are assumed to be caused by the larger, less compact molecular shapes of alkyl OPs as observed for other unbranched alkyl compounds previously<sup>48</sup>. Additionally, we report and compare  $^{DT}CCS_{N2}$  values of common isomers of OPs and two isomeric metabolites for the first time. The  $^{DT}CCS_{N2}$  values acquired for three isomers of tricresyl phosphate (TCP), two isomers of tributyl phosphate (TBP) and the hydroxylated metabolites 3OH-TPHP and 4OH-TPHP are given in Table 2. Based on the observed low RSDs (range 0.02% to 0.14%) which indicate the high reproducibility of the acquired values, the reported data will allow isomer identification. This will also be demonstrated for the isomeric metabolites in urine samples (see below). In previous studies, the separation between the isomers of TCP and TBP was achieved when gas chromatography was used<sup>51, 52</sup>. However, most biomonitoring methods apply liquid chromatography and lack a distinction between the different isomers of TCP, therefore reporting total TCP concentrations<sup>53, 54</sup> or investigating only one of the TBP isomers<sup>55</sup>. Yet, within the endocrine-disrupting effects reported for TCPs, different modes of actions have been recently reported for the three isomers, indicating a growing need for a distinction between them<sup>56</sup>. The reported data will serve as a valuable tool to achieve this distinction in future studies.

**Table 2:** CCS values of isomeric organophosphorus flame retardants and two of their metabolites.

Compound	Abbreviation	<i>m/z</i>	Ion	$^{DT}CCS_{N2}$ ( $\pm$ SD) [ $\text{\AA}^2$ ]	RSD [%]
Triisobutyl phosphate	TiBP	267.1720	[M+H] <sup>+</sup>	165.44 (0.23)	0.14
		289.1539	[M+Na] <sup>+</sup>	183.19 (0.08)	0.04
		533.3367	[2M+H] <sup>+</sup>	234.54 (0.09)	0.04
		555.3186	[2M+Na] <sup>+</sup>	248.38 (0.12)	0.05
Tri- <i>n</i> -butyl phosphate	TnBP	267.1720	[M+H] <sup>+</sup>	166.73 (0.06)	0.03
		289.1539	[M+Na] <sup>+</sup>	184.54 (0.10)	0.05
		533.3367	[2M+H] <sup>+</sup>	236.49 (0.09)	0.04
		555.3186	[2M+Na] <sup>+</sup>	250.03 (0.12)	0.05
Tri- <i>m</i> -tolyl phosphate	TMTP	369.1250	[M+H] <sup>+</sup>	188.56 (0.10)	0.06
		391.1070	[M+Na] <sup>+</sup>	198.56 (0.12)	0.06
		759.2247	[2M+Na] <sup>+</sup>	272.51 (0.16)	0.06
Tri- <i>o</i> -tolyl phosphate	TOTP	369.1250	[M+H] <sup>+</sup>	182.39 (0.08)	0.04
		391.1070	[M+Na] <sup>+</sup>	192.43 (0.16)	0.08
		759.2247	[2M+Na] <sup>+</sup>	263.75 (0.20)	0.08
Tri- <i>p</i> -tolyl phosphate	TPTP	369.1250	[M+H] <sup>+</sup>	190.02 (0.06)	0.03
		391.1070	[M+Na] <sup>+</sup>	200.02 (0.08)	0.04
		759.2247	[2M+Na] <sup>+</sup>	273.74 (0.13)	0.05
3-Hydroxyphenyl diphenyl phosphate	3OH-TPHP*	341.0584	[M-H] <sup>-</sup>	180.46 (0.10)	0.06
4-Hydroxyphenyl diphenyl phosphate	4OH-TPHP*	341.0584	[M-H] <sup>-</sup>	181.90 (0.05)	0.03

\*=compounds were also detected in ESI+, the data can be found in Table S5 and Table S6.

The  $^{DT}CCS_{N2}$  values acquired for plasticizers were also well fitted using a power model (see Figure 1C) showing a correlation coefficient of  $R^2 = 0.952$ . To improve the overview, several compound classes (i.e. phthalates, terephthalates, adipates and their metabolites, respectively, as well as trimellitates, citrates and a derivative of azelate) were included in the plot of plasticizers. However, only four compounds showed clear deviations from the

302 trendline. These included tri-*n*-hexyltrimellitate (THTM) and tris(2-ethylhexyl)-trimellitate (TOTM) which showed a  
303 shift towards higher  $^{DT}CCS_{N2}$  values, as well as diphenyl phthalate (DPP) and acetyltriethyl citrate (ATEC) shifting  
304 towards lower  $^{DT}CCS_{N2}$ . THTM and TOTM are the only two trimellitates investigated in this study. They consist of  
305 a trimellitic acid backbone which is fully esterified resulting in a large size molecule and thereof decreased ion  
306 mobility and increased  $^{DT}CCS_{N2}$  value. In contrast, DPP was the only aryl phthalate ester investigated. Similar to  
307 the effects observed for OP aryl triesters, the compact phenyl residues lead to a smaller molecular size in  
308 comparison with the other (alkyl) phthalates. Comparable effects were observed for ATEC which in contrast to the  
309 other citrates investigated (i.e. butyryl trihexyl citrate and tributyl acetylcitrate) showed the most compact  
310 sidechains. However, this cannot fully explain the observed shifts as the described substituents of DPP and ATEC  
311 did not have a visible influence on the  $^{DT}CCS_{N2}$  values of the monomer ions. Molecular modeling studies are  
312 needed to further investigate possible conformational changes or intramolecular interactions between monomer  
313 and dimer ions of ATEC and DPP. To our knowledge, it is the first time that  $^{DT}CCS_{N2}$  values for a high variety of  
314 plasticizer classes and their most important metabolites are reported. Due to the low mass range investigated  
315 here, the coelution of interfering matrix components is a common problem leading to a high number of false  
316 positives<sup>57, 58</sup>, and the reported data can serve as an additional identification tool to reach higher levels of certainty  
317 within compound identification.

318 The PFAS investigated in this study included a set of perfluoroalkyl carboxylic and sulfonic acids (PFCA and PFSA,  
319 respectively) as well as a selection of emerging PFAS, such as three fluorotelomer sulfonic acids (FTSA), *N*-  
320 alkylated perfluorooctanesulfonamides and others (Table S5). The high number of CF<sub>2</sub> moieties incorporated in  
321 these compounds leads to increased molecular masses and thereof decreased  $^{DT}CCS_{N2}$  values in relation to the  
322 *m/z* ratios. This results in a lower slope of the observed trendline (see Figure 1D) allowing a clear distinction  
323 between PFAS and the other compound classes investigated in this study. Even though the investigated emerging  
324 PFAS varied in molecular composition (e.g. *N*-alkyl or chlorinated derivatives), no characteristic deviations from  
325 the calculated dependence were observed leading to a high correlation coefficient of  $R^2 = 0.979$ . The different  
326 trendlines observed for individual PFAS subclasses have been discussed in detail previously<sup>35, 37</sup> and therefore  
327 were not further characterized here. However, in order to show high (interlaboratory) repeatability of the acquired  
328 data as well as the characteristic linear correlation between  $^{DT}CCS_{N2}$  and *m/z* values of PFCA, Figure 1D  
329 additionally shows the linear trendline of the [M-H-CO<sub>2</sub>]<sup>-</sup> ions of PFCAs of different chain lengths. The high linear  
330 correlation ( $R^2 = 0.999$ ) is in line with the observations from a previous study<sup>35</sup>. In addition,  $^{DT}CCS_{N2}$  values of  
331 twelve emerging PFAS and the [M+H]<sup>+</sup> ions of two PFCAs are reported for the first time.

332 Overall, the  $^{DT}CCS_{N2}$  database compiled within this study yielded 113 compounds for which  $^{DT}CCS_{N2}$  values were  
333 described for the first time, presenting a breakthrough towards a wide application of DTIMS for CECs analysis.

334

### 335 **Comparison with literature $^{DT}CCS_{N2}$ and $^{TW}CCS_{N2}$ values**

336 To evaluate the accuracy of the  $^{DT}CCS_{N2}$  values included in the database and their “between-laboratory”  
337 reproducibility, our data was compared with  $^{DT}CCS_{N2}$  and  $^{TW}CCS_{N2}$  values available in the literature. Several  
338  $^{DT}CCS_{N2}$  and  $^{TW}CCS_{N2}$  databases were searched for reference values of the compounds described in this study<sup>20</sup>,

21, 23, 35, 38-40, 42. Only a limited number of literature values are available, (partly) covering only two compound classes investigated in this study, i.e. PFAS<sup>35</sup> and OPs<sup>38</sup>, and providing a reference  $^{DT}CCS_{N_2}$  for di(2-ethylhexyl) phthalate (DEHP)<sup>42</sup>. In the cited studies, CCS values for PFAS and DEHP were acquired using DTIMS, whereas OPs were analyzed using traveling wave ion mobility spectrometry (TWIMS), respectively. Table S7 shows a comparison of literature IM-MS data with the  $^{DT}CCS_{N_2}$  values acquired in our study.

For  $^{TW}CCS_{N_2}$  values for OPs in comparison to our data, the absolute percent errors (APE) ranged from 0.13% (for TCIPP) and 2.85% (for TPHP), with an average APE of 1.03%.  $^{DT}CCS_{N_2}$  values for PFAS showed an APE of 0.28%. Thereby, the highest absolute percent error with 1.15% was observed for the  $[M-H-CO_2]^-$  ion of perfluoro-*n*-butanoic acid (PFBA) and the lowest of 0.02% corresponded to the  $[M-H]^-$  ion of perfluoro-*n*-undecanoic acid (PFUdA). Similar values were observed for the comparison of  $^{DT}CCS_{N_2}$  values of DEHP (APE of 0.57% for  $[M+H]^+$  and 0.26% for  $[M+Na]^+$ , respectively). The low average percent error observed for the comparison of DTIMS data is in agreement with values reported in previous studies investigating inter-laboratory reproducibility  $^{DT}CCS_{N_2}$  values<sup>21, 22</sup>. The high percent error observed for PFBA most probably results from its low *m/z* (*m/z* 168.9894) which leads to an increased percent error, while the absolute deviation in  $^{DT}CCS_{N_2}$  is comparable with other PFAS compounds ( $\Delta^{DT}CCS_{N_2} = -1.27 \text{ \AA}^2$ ).

When comparing TWIMS data of OPs with the  $^{DT}CCS_{N_2}$  values of our database, the different calibration and acquisition principles of these techniques, which might lead to increased deviations have to be considered: Unlike DTIMS, a constantly varying electrical field used in TWIMS makes it impossible to directly derive the CCS value of a compound from its reduced mobility ( $K_0$ )<sup>32</sup>. Therefore, a set of calibration standards with known CCS values derived from drift tube measurements is needed. Consequently, deviations of up to 6.2% between TWIMS and DTIMS data have been observed previously<sup>59</sup>. The mentioned differences between these two techniques are also assumed to cause the increased average error observed here. Hence, when applying the database introduced here for TWIMS measurements, an in-depth evaluation of the measurement deviations and, if necessary, the use of higher tolerance windows within suspect screening methods are advised.

### Application of the $^{DT}CCS_{N_2}$ database to human urine samples

To evaluate the applicability of our  $^{DT}CCS_{N_2}$  database to human urine samples, pooled urine samples were spiked with a set of 15 AP and 15 OP metabolites at two concentration levels (20 ng/mL and 50 ng/mL). After sample preparation (which included a dilution with a factor of 5) and analysis, 13 out of 15 OP metabolites were detected in spiked urine samples and their average  $^{DT}CCS_{N_2}$  and mass errors were calculated (see Table S8). For all detected OP metabolites, the APEs of  $^{DT}CCS_{N_2}$  values observed in urine (in comparison to database values) were <1% ranging from 0.02% to 0.74% and showing an average of 0.12% for the higher and 0.15% for the lower concentration level, respectively. Bis(2-chloropropyl) hydrogen phosphate (BCIPP) and bis(2-chloroethyl) phosphate (BCEP) were not detected at either of the concentration levels, in accordance with a previous study in which BCEP and BCIPP showed the highest detection limits<sup>45</sup>.

For AP metabolites, 11 out of their 15 metabolites were detected at both concentration levels (Table S9). Mono(2-ethyl-5-carboxypentyl) terephthalate (5-cx-MEPTP) was only detected at 50 ng/mL. The observed APEs ranged

from <0.01% to 0.42% showing and an average percent error of 0.09% for the lower and 0.10% for the higher concentration level, respectively. These similar results indicate that the reproducibility of <sup>DT</sup>CCS<sub>N2</sub> in human samples is not influenced by the concentration level. However, for a few AP metabolites an optimized chromatographic approach is needed to detect them at these concentration levels.

Overall, it can be concluded that the <sup>DT</sup>CCS<sub>N2</sub> database compiled in this study provides reliable data to be applied to human samples and can serve as a valuable additional tool for CEC identification in future suspect screening studies. Furthermore, the observed deviations of <sup>DT</sup>CCS<sub>N2</sub> values in spiked urine samples were clearly below the threshold of 2% recently proposed for reporting compound identification levels derived from IM-HRMS data<sup>40</sup>.

In conclusion, the database provided in this study incorporates a high number and variety of CEC classes. Based on the implemented strict and comprehensive QA guidelines, we are convinced that it can serve as a valuable complementary tool in future studies allowing to further exploit the high potential of IM-MS data as a unique molecular descriptor.

## Acknowledgments

Drs. L. Belova acknowledges funding through a Research Foundation Flanders (FWO) fellowship (11G1821N). Dr. N. Caballero-Casero acknowledges a postdoctoral fellowship from the University of Antwerp. This work was supported by the Exposome Centre of Excellence of the University of Antwerp (BOF grant, Antigoon database number 41222).

## Supporting information

Information on the investigated compound classes, applied drift tube settings, chromatographic method for PFAS analysis, CCS values of QA compounds in comparison with literature data, complete CCS database of 148 compounds, comparison of experimental CCS values with literature data, reproducibility of CCS values of OP and AP metabolites in pooled human urine samples. (PDF)

Complete CCS database for 311 ions of 148 compounds. (CSV and XSLX)

## References

1. Tang, B.; Christia, C.; Malarvannan, G.; Liu, Y. E.; Luo, X. J.; Covaci, A.; Mai, B. X.; Poma, G., Legacy and emerging organophosphorus flame retardants and plasticizers in indoor microenvironments from Guangzhou, South China. *Environ Int* **2020**, *143*, 105972.
2. He, K.; Hain, E.; Timm, A.; Tarnowski, M.; Blaney, L., Occurrence of antibiotics, estrogenic hormones, and UV-filters in water, sediment, and oyster tissue from the Chesapeake Bay. *Sci Total Environ* **2019**, *650* (Pt 2), 3101-3109.
3. Ballesteros-Gomez, A.; Ballesteros, J.; Ortiz, X.; Jonker, W.; Helmus, R.; Jobst, K. J.; Parsons, J. R.; Reiner, E. J., Identification of Novel Brominated Compounds in Flame Retarded Plastics Containing TBBPA by Combining Isotope Pattern and Mass Defect Cluster Analysis. *Environ Sci Technol* **2017**, *51* (3), 1518-1526.
4. Sauve, S.; Desrosiers, M., A review of what is an emerging contaminant. *Chem Cent J* **2014**, *8* (1), 15.
5. Pourchet, M.; Debrauwer, L.; Klanova, J.; Price, E. J.; Covaci, A.; Caballero-Casero, N.; Oberacher, H.; Lamoree, M.; Damont, A.; Fenaille, F.; Vlaanderen, J.; Meijer, J.; Krauss, M.; Sarigiannis, D.; Barouki, R.; Le Bizec, B.; Antignac, J. P., Suspect and non-targeted screening of chemicals of emerging concern for human biomonitoring, environmental health studies and support to risk assessment: From promises to challenges and harmonisation issues. *Environ Int* **2020**, *139*, 105545.

6. Andra, S. S.; Austin, C.; Patel, D.; Dolios, G.; Awawda, M.; Arora, M., Trends in the application of high-resolution mass spectrometry for human biomonitoring: An analytical primer to studying the environmental chemical space of the human exposome. *Environ Int* **2017**, *100*, 32-61.
7. Dennis, K. K.; Marder, E.; Balshaw, D. M.; Cui, Y.; Lynes, M. A.; Patti, G. J.; Rappaport, S. M.; Shaughnessy, D. T.; Vrijheid, M.; Barr, D. B., Biomonitoring in the Era of the Exposome. *Environ Health Perspect* **2017**, *125* (4), 502-510.
8. Tian, Z.; Peter, K. T.; Gipe, A. D.; Zhao, H.; Hou, F.; Wark, D. A.; Khangaonkar, T.; Kolodziej, E. P.; James, C. A., Suspect and Nontarget Screening for Contaminants of Emerging Concern in an Urban Estuary. *Environ Sci Technol* **2020**, *54* (2), 889-901.
9. Hollender, J.; Schymanski, E. L.; Singer, H. P.; Ferguson, P. L., Nontarget Screening with High Resolution Mass Spectrometry in the Environment: Ready to Go? *Environ Sci Technol* **2017**, *51* (20), 11505-11512.
10. Schymanski, E. L.; Jeon, J.; Gulde, R.; Fenner, K.; Ruff, M.; Singer, H. P.; Hollender, J., Identifying small molecules via high resolution mass spectrometry: communicating confidence. *Environ Sci Technol* **2014**, *48* (4), 2097-8.
11. Oberacher, H.; Sasse, M.; Antignac, J.-P.; Guitton, Y.; Debrauwer, L.; Jamin, E. L.; Schulze, T.; Krauss, M.; Covaci, A.; Caballero-Casero, N.; Rousseau, K.; Damont, A.; Fenaille, F.; Lamoree, M.; Schymanski, E. L., A European proposal for quality control and quality assurance of tandem mass spectral libraries. *Environmental Sciences Europe* **2020**, *32* (1).
12. Guo, Z.; Huang, S.; Wang, J.; Feng, Y. L., Recent advances in non-targeted screening analysis using liquid chromatography - high resolution mass spectrometry to explore new biomarkers for human exposure. *Talanta* **2020**, *219*, 121339.
13. Chouinard, C. D.; Beekman, C. R.; Kemperman, R. H. J.; King, H. M.; Yost, R. A., Ion mobility-mass spectrometry separation of steroid structural isomers and epimers. *International Journal for Ion Mobility Spectrometry* **2016**, *20* (1-2), 31-39.
14. Lanucara, F.; Holman, S. W.; Gray, C. J.; Evers, C. E., The power of ion mobility-mass spectrometry for structural characterization and the study of conformational dynamics. *Nat Chem* **2014**, *6* (4), 281-94.
15. Causon, T. J.; Si-Hung, L.; Newton, K.; Kurulugama, R. T.; Fjeldsted, J.; Hann, S., Fundamental study of ion trapping and multiplexing using drift tube-ion mobility time-of-flight mass spectrometry for non-targeted metabolomics. *Anal Bioanal Chem* **2019**, *411* (24), 6265-6274.
16. May, J. C.; Knochenmuss, R.; Fjeldsted, J. C.; McLean, J. A., Resolution of Isomeric Mixtures in Ion Mobility Using a Combined Demultiplexing and Peak Deconvolution Technique. *Anal Chem* **2020**, *92* (14), 9482-9492.
17. Ewing, M. A.; Glover, M. S.; Clemmer, D. E., Hybrid ion mobility and mass spectrometry as a separation tool. *J Chromatogr A* **2016**, *1439*, 3-25.
18. Metz, T. O.; Baker, E. S.; Schymanski, E. L.; Renslow, R. S.; Thomas, D. G.; Causon, T. J.; Webb, I. K.; Hann, S.; Smith, R. D.; Teeguarden, J. G., Integrating ion mobility spectrometry into mass spectrometry-based exposome measurements: what can it add and how far can it go? *Bioanalysis* **2017**, *9* (1), 81-98.
19. Goscinny, S.; McCullagh, M.; Far, J.; De Pauw, E.; Eppe, G., Towards the use of ion mobility mass spectrometry derived collision cross section as a screening approach for unambiguous identification of targeted pesticides in food. *Rapid Commun Mass Spectrom* **2019**, *33* Suppl 2, 34-48.
20. Tejada-Casado, C.; Hernandez-Mesa, M.; Monteau, F.; Lara, F. J.; Olmo-Iruela, M. D.; Garcia-Campana, A. M.; Le Bizec, B.; Dervilly-Pinel, G., Collision cross section (CCS) as a complementary parameter to characterize human and veterinary drugs. *Anal Chim Acta* **2018**, *1043*, 52-63.
21. Picache, J. A.; Rose, B. S.; Balinski, A.; Leaptrot, K. L.; Sherrod, S. D.; May, J. C.; McLean, J. A., Collision cross section compendium to annotate and predict multi-omic compound identities. *Chem Sci* **2019**, *10* (4), 983-993.
22. Stow, S. M.; Causon, T. J.; Zheng, X.; Kurulugama, R. T.; Mairinger, T.; May, J. C.; Rennie, E. E.; Baker, E. S.; Smith, R. D.; McLean, J. A.; Hann, S.; Fjeldsted, J. C., An Interlaboratory Evaluation of Drift Tube Ion Mobility-Mass Spectrometry Collision Cross Section Measurements. *Anal Chem* **2017**, *89* (17), 9048-9055.
23. Hines, K. M.; Ross, D. H.; Davidson, K. L.; Bush, M. F.; Xu, L., Large-Scale Structural Characterization of Drug and Drug-Like Compounds by High-Throughput Ion Mobility-Mass Spectrometry. *Anal Chem* **2017**, *89* (17), 9023-9030.
24. Regueiro, J.; Negreira, N.; Berntssen, M. H., Ion-Mobility-Derived Collision Cross Section as an Additional Identification Point for Multiresidue Screening of Pesticides in Fish Feed. *Anal Chem* **2016**, *88* (22), 11169-11177.
25. Lietz, C. B.; Yu, Q.; Li, L., Large-scale collision cross-section profiling on a traveling wave ion mobility mass spectrometer. *J Am Soc Mass Spectrom* **2014**, *25* (12), 2009-19.
26. Struwe, W. B.; Pagel, K.; Benesch, J. L.; Harvey, D. J.; Campbell, M. P., GlycoMob: an ion mobility-mass spectrometry collision cross section database for glycomics. *Glycoconj J* **2016**, *33* (3), 399-404.
27. Hines, K. M.; Herron, J.; Xu, L., Assessment of altered lipid homeostasis by HILIC-ion mobility-mass spectrometry-based lipidomics. *J Lipid Res* **2017**, *58* (4), 809-819.
28. Hernandez-Mesa, M.; Le Bizec, B.; Monteau, F.; Garcia-Campana, A. M.; Dervilly-Pinel, G., Collision Cross Section (CCS) Database: An Additional Measure to Characterize Steroids. *Anal Chem* **2018**, *90* (7), 4616-4625.
29. Lacalle-Bergeron, L.; Portoles, T.; Lopez, F. J.; Sancho, J. V.; Ortega-Azorin, C.; Asensio, E. M.; Coltell, O.; Corella, D., Ultra-Performance Liquid Chromatography-Ion Mobility Separation-Quadrupole Time-of-Flight MS (UHPLC-IMS-QTOF MS) Metabolomics for Short-Term Biomarker Discovery of Orange Intake: A Randomized, Controlled Crossover Study. *Nutrients* **2020**, *12* (7).
30. Luo, M.-D.; Zhou, Z.-W.; Zhu, Z.-J., The Application of Ion Mobility-Mass Spectrometry in Untargeted Metabolomics: from Separation to Identification. *Journal of Analysis and Testing* **2020**, *4* (3), 163-174.
31. George, A. D.; Gay, M. C. L.; Wlodek, M. E.; Trengove, R. D.; Murray, K.; Geddes, D. T., Untargeted lipidomics using liquid chromatography-ion mobility-mass spectrometry reveals novel triacylglycerides in human milk. *Sci Rep* **2020**, *10* (1), 9255.

32. Hines, K. M.; May, J. C.; McLean, J. A.; Xu, L., Evaluation of Collision Cross Section Calibrants for Structural Analysis of Lipids by Traveling Wave Ion Mobility-Mass Spectrometry. *Anal Chem* **2016**, *88* (14), 7329-36.
33. Wang, Y.; de, B. H. P.; Chang, T.; Wu, X.; Chen, P., Analysis of cranberry proanthocyanidins using UPLC-ion mobility-high-resolution mass spectrometry. *Anal Bioanal Chem* **2020**, *412* (15), 3653-3662.
34. Nys, G.; Nix, C.; Cobraiville, G.; Servais, A. C.; Fillet, M., Enhancing protein discoverability by data independent acquisition assisted by ion mobility mass spectrometry. *Talanta* **2020**, *213*, 120812.
35. Dodds, J. N.; Hopkins, Z. R.; Knappe, D. R. U.; Baker, E. S., Rapid Characterization of Per- and Polyfluoroalkyl Substances (PFAS) by Ion Mobility Spectrometry-Mass Spectrometry (IMS-MS). *Anal Chem* **2020**, *92* (6), 4427-4435.
36. Yukioka, S.; Tanaka, S.; Suzuki, Y.; Fujii, S.; Echigo, S., A new method to search for per- and polyfluoroalkyl substances (PFASs) by linking fragmentation flags with their molecular ions by drift time using ion mobility spectrometry. *Chemosphere* **2020**, *239*, 124644.
37. Ahmed, E.; Mohibul Kabir, K. M.; Wang, H.; Xiao, D.; Fletcher, J.; Donald, W. A., Rapid separation of isomeric perfluoroalkyl substances by high-resolution differential ion mobility mass spectrometry. *Anal Chim Acta* **2019**, *1058*, 127-135.
38. Mullin, L.; Jobst, K.; DiLorenzo, R. A.; Plumb, R.; Reiner, E. J.; Yeung, L. W. Y.; Jogsten, I. E., Liquid chromatography-ion mobility-high resolution mass spectrometry for analysis of pollutants in indoor dust: Identification and predictive capabilities. *Anal Chim Acta* **2020**, *1125*, 29-40.
39. Zheng, X.; Aly, N. A.; Zhou, Y.; Dupuis, K. T.; Bilbao, A.; Paurus, V. L.; Orton, D. J.; Wilson, R.; Payne, S. H.; Smith, R. D.; Baker, E. S., A structural examination and collision cross section database for over 500 metabolites and xenobiotics using drift tube ion mobility spectrometry. *Chem Sci* **2017**, *8* (11), 7724-7736.
40. Celma, A.; Sancho, J. V.; Schymanski, E. L.; Fabregat-Safont, D.; Ibanez, M.; Goshawk, J.; Barknowitz, G.; Hernandez, F.; Bijlsma, L., Improving Target and Suspect Screening High-Resolution Mass Spectrometry Workflows in Environmental Analysis by Ion Mobility Separation. *Environ Sci Technol* **2020**, *54* (23), 15120-15131.
41. Mordehai, A.; Kurulugama, R. T.; Darland, E.; Stafford, G.; Fjeldsted, J. C., Single Field Direct Drift Time to CCS Calibration for a Linear Drift Tube Ion Mobility Mass Spectrometer. *ASMS, Agilent Technologies* **2015**, 1-4.
42. Nichols, C. M.; Dodds, J. N.; Rose, B. S.; Picache, J. A.; Morris, C. B.; Codreanu, S. G.; May, J. C.; Sherrod, S. D.; McLean, J. A., Untargeted Molecular Discovery in Primary Metabolism: Collision Cross Section as a Molecular Descriptor in Ion Mobility-Mass Spectrometry. *Anal Chem* **2018**, *90* (24), 14484-14492.
43. Prost, S. A.; Crowell, K. L.; Baker, E. S.; Ibrahim, Y. M.; Clowers, B. H.; Monroe, M. E.; Anderson, G. A.; Smith, R. D.; Payne, S. H., Detecting and removing data artifacts in Hadamard transform ion mobility-mass spectrometry measurements. *J Am Soc Mass Spectrom* **2014**, *25* (12), 2020-2027.
44. Deventer, K.; Pozo, O. J.; Verstraete, A. G.; Van Eenoo, P., Dilute-and-shoot-liquid chromatography-mass spectrometry for urine analysis in doping control and analytical toxicology. *TrAC Trends in Analytical Chemistry* **2014**, *55*, 1-13.
45. Bastiaensen, M.; Xu, F.; Been, F.; Van den Eede, N.; Covaci, A., Simultaneous determination of 14 urinary biomarkers of exposure to organophosphate flame retardants and plasticizers by LC-MS/MS. *Anal Bioanal Chem* **2018**, *410* (30), 7871-7880.
46. Zheng, X.; Dupuis, K. T.; Aly, N. A.; Zhou, Y.; Smith, F. B.; Tang, K.; Smith, R. D.; Baker, E. S., Utilizing ion mobility spectrometry and mass spectrometry for the analysis of polycyclic aromatic hydrocarbons, polychlorinated biphenyls, polybrominated diphenyl ethers and their metabolites. *Anal Chim Acta* **2018**, *1037*, 265-273.
47. Chouinard, C. D.; Cruzeiro, V. W. D.; Roitberg, A. E.; Yost, R. A., Experimental and Theoretical Investigation of Sodiated Multimers of Steroid Epimers with Ion Mobility-Mass Spectrometry. *J Am Soc Mass Spectrom* **2017**, *28* (2), 323-331.
48. May, J. C.; Goodwin, C. R.; Lareau, N. M.; Leaptrot, K. L.; Morris, C. B.; Kurulugama, R. T.; Mordehai, A.; Klein, C.; Barry, W.; Darland, E.; Overney, G.; Imatani, K.; Stafford, G. C.; Fjeldsted, J. C.; McLean, J. A., Conformational ordering of biomolecules in the gas phase: nitrogen collision cross sections measured on a prototype high resolution drift tube ion mobility-mass spectrometer. *Anal Chem* **2014**, *86* (4), 2107-16.
49. Tao, L.; McLean, J. R.; McLean, J. A.; Russell, D. H., A collision cross-section database of singly-charged peptide ions. *J Am Soc Mass Spectrom* **2007**, *18* (7), 1232-8.
50. Esquenazi, E.; Daly, M.; Bahrainwala, T.; Gerwick, W. H.; Dorrestein, P. C., Ion mobility mass spectrometry enables the efficient detection and identification of halogenated natural products from cyanobacteria with minimal sample preparation. *Bioorg Med Chem* **2011**, *19* (22), 6639-44.
51. Van den Eede, N.; Dirtu, A. C.; Ali, N.; Neels, H.; Covaci, A., Multi-residue method for the determination of brominated and organophosphate flame retardants in indoor dust. *Talanta* **2012**, *89*, 292-300.
52. Lee, H. K.; Kang, H.; Lee, S.; Kim, S.; Choi, K.; Moon, H. B., Human exposure to legacy and emerging flame retardants in indoor dust: A multiple-exposure assessment of PBDEs. *Sci Total Environ* **2020**, *719*, 137386.
53. Bastiaensen, M.; Ait Bamai, Y.; Araki, A.; Van den Eede, N.; Kawai, T.; Tsuboi, T.; Kishi, R.; Covaci, A., Biomonitoring of organophosphate flame retardants and plasticizers in children: Associations with house dust and housing characteristics in Japan. *Environ Res* **2019**, *172*, 543-551.
54. Christia, C.; Poma, G.; Besis, A.; Samara, C.; Covaci, A., Legacy and emerging organophosphomicrocrystalline flame retardants in car dust from Greece: Implications for human exposure. *Chemosphere* **2018**, *196*, 231-239.
55. Ding, J.; Xu, Z.; Huang, W.; Feng, L.; Yang, F., Organophosphate ester flame retardants and plasticizers in human placenta in Eastern China. *Sci Total Environ* **2016**, *554-555*, 211-7.
56. Ji, X.; Li, N.; Ma, M.; Rao, K.; Yang, R.; Wang, Z., Tricresyl phosphate isomers exert estrogenic effects via G protein-coupled estrogen receptor-mediated pathways. *Environ Pollut* **2020**, *264*, 114747.

- 539 57. Crowell, K. L.; Baker, E. S.; Payne, S. H.; Ibrahim, Y. M.; Monroe, M. E.; Slys, G. W.; LaMarche, B. L.; Petyuk, V. A.;  
540 Piehowski, P. D.; Danielson, W. F., 3rd; Anderson, G. A.; Smith, R. D., Increasing Confidence of LC-MS Identifications by  
541 Utilizing Ion Mobility Spectrometry. *Int J Mass Spectrom* **2013**, 354-355, 312-317.
- 542 58. Gerona, R. R.; Schwartz, J. M.; Pan, J.; Friesen, M. M.; Lin, T.; Woodruff, T. J., Suspect screening of maternal serum to  
543 identify new environmental chemical biomonitoring targets using liquid chromatography-quadrupole time-of-flight mass  
544 spectrometry. *J Expo Sci Environ Epidemiol* **2018**, 28 (2), 101-108.
- 545 59. Hinnenkamp, V.; Klein, J.; Meckelmann, S. W.; Balsaa, P.; Schmidt, T. C.; Schmitz, O. J., Comparison of CCS Values  
546 Determined by Traveling Wave Ion Mobility Mass Spectrometry and Drift Tube Ion Mobility Mass Spectrometry. *Anal Chem*  
547 **2018**, 90 (20), 12042-12050.

548